

Electronic properties of mixed valence iron(II,III) dinuclear complexes with carboxylate bridges

V. Paredes-García^{a,b,*}, D. Venegas-Yazigi^a, R.O. Latorre^a, E. Spodine^a

^a Centro para la Investigación Interdisciplinaria Avanzada en Ciencias de los Materiales (CIMAT), Facultad de Ciencias Químicas y Farmacéuticas, U. de Chile, Olivos 1007, Casilla 233, Santiago, Chile

^b Departamento de Química, Facultad de Ciencias Naturales, Matemáticas y del Medio Ambiente, Universidad Tecnológica Metropolitana, Av. José Pedro Alessandri 1242, Santiago, Chile

Abstract

Mixed valence dinuclear iron(II,III) complexes of the type $[\text{Fe}_2\text{L}_2(\text{H}_2\text{O})_4](\text{NO}_3)(\text{H}_2\text{O})_3$, where L is the dianion of a Schiff base ligand derived from α -amino acids (glycine and L-isoleucine) and 5-bromosalicylaldehyde, have been prepared and characterised using different spectroscopic methods, magnetic susceptibility, conductivity, and electrochemical measurements. The mixed valence iron complexes can be described as hexacoordinated species, in which the metal ion is surrounded by water molecules, the salicylidenimine ligand and two bridging carboxylate groups. The presence of bromine as a substituent in the salicylaldehyde ring stabilises the mixed valence species.

Keywords: Schiff base metal complexes; Mixed-valence dinuclear iron(II,III) complexes; Carboxylate bridging ligands; ^{57}Fe Mössbauer spectroscopy; Variable-temperature magnetic susceptibility studies; Cyclic voltammetry

1. Introduction

An important class of metalloproteins is that which contains carboxylate-bridged diiron cores, which perform a variety of different functions in biological systems in spite of their structural similarities. For example carboxylate-bridged diiron centres activate dioxygen for radical generation and hydrocarbon oxidation at the active sites of enzymes such as ribonucleotide reductase (RNR-R2), soluble methane monooxygenase hydroxylase (sMMOH) and desaturase ($\Delta^9\text{D}$) [1–4]. On the other hand, haemerythrins (Hr) are dioxygen carrier proteins found in marine invertebrates that are functional analogues of the mammalian proteins myoglobin and haemoglobin [5]. Furthermore, the metalloproteins having Fe(II,III) sites are important participants in biological electron transfer reactions [6,7].

The development of synthetic small molecules as model compounds for dinuclear iron-based complexes with carboxylate bridges has received considerable attention due to their importance as structural, spectroscopic and functional models of the active sites of these proteins [1–3]. How a protein defines the properties of the metal ions, as well as the selectivity and efficiency of the reactions that involve such metal ions, has been investigated with biomimetic inorganic compounds in recent years [1–3]. The design and synthesis of organic precursors with suitable dinucleating character can therefore be crucial to obtain these biometric compounds. The ligands should bridge the metal ions, preferably through a carboxylate unit, and thus produce dinuclear, rather than mono- or polynuclear species [8].

On the other hand, the coordination number of each iron atom in the resulting compound is also important, since it is desirable that a diiron complex should react with different substrates coordinated to the metal centre. Consequently, these compounds should either be coordinatively

* Corresponding author. Tel.: +562 9782801, fax: +562 9782868.
E-mail address: fqi@ciq.uchile.cl (V. Paredes-García).

unsaturated, or contain readily exchangeable ligands, such as water or other solvent components [5].

The use of amino acid-derived Schiff bases as model systems has been mainly justified by the participation of these ligands in similar biological compounds in key biological reactions [2–10]. The magnetic, electrochemical and spectroscopic studies of the synthetic systems provide important information about redox and spin states of the metal centre(s), the magnitude of the exchange interaction, and the coordination environment which has a profound influence on the functional properties of the complexes. These models also allow structure and the magnetic, electronic, and optical properties of the metal sites present in biological systems to be correlated [11–15].

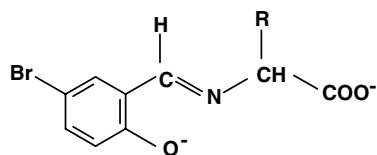
In a recent paper on $\text{Fe}_2(\mu\text{-carboxylate})_2(\text{L}_2)_2$ complexes, where L is a Schiff base derived from an α -amino acid and salicylaldehyde, we postulated that the dimeric iron(III) complexes are hexacoordinated, the metal ion being surrounded by water molecules, the salicylideneimine ligand and bridging carboxylate groups [16]. In this work, we report the synthesis of mixed valence dinuclear iron(II,III) complexes of the type $[\text{Fe}_2\text{L}_2(\text{H}_2\text{O})_4](\text{NO}_3)(\text{H}_2\text{O})_3$, where L is a Schiff base derived from an α -amino acids (glycine or L-isoleucine) and 5-bromosalicylaldehyde (Fig. 1). We have characterised these complexes using different spectroscopic techniques, plus magnetic susceptibility, conductivity, and electrochemical measurements.

2. Experimental

The reagents 5-bromosalicylaldehyde, glycine (Gly) and L-isoleucine (Ile) were purchased from Merck (analytical grade) and were used without further purification.

The ligands were synthesised as described by Paredes et al. [16] (yields 73–85%). Both ligands synthesised by this method are solids and were isolated as potassium salts. They were characterised by elemental analysis, and FTIR, UV–Vis and ^1H NMR spectroscopic methods.

The mixed valence complexes were prepared as described by Casella et al. [17]. The ligand (1 mmol) was dissolved in methanol at room temperature, and 1 mmol of potassium hydroxide was added. Finally, $\text{Fe}(\text{NO}_3)_3 \cdot 9\text{H}_2\text{O}$ (1 mmol), was added directly to the solution. The reaction mixture was left for 5–6 h at room temperature with continuous stirring under nitrogen. The KNO_3 formed was filtered off and the solution was concentrated; the product was precipitated with *n*-hexane and was dried under vacuum.



R = H, N-5-bromosalicylidene-glycine
R = *sec*-Bu, N-5-bromosalicylidene-isoleucine

Fig. 1. Structural formulae for Schiff base ligands (L^{2-}) derived from glycine, isoleucine and 5-bromosalicylaldehyde.

initiated with *n*-hexane and was dried under vacuum. The complexes synthesised by this method are dark violet amorphous solids with molecular formulae $[\text{Fe}_2\text{L}_2(\text{H}_2\text{O})_4](\text{NO}_3)(\text{H}_2\text{O})_3$ (yields 60–70%). In general, the complexes are highly insoluble in most low-polarity organic solvents and, unfortunately, single crystals suitable for X-ray diffraction were not obtained.

$[\text{Fe}_2(\text{BrSA-Gly})_2(\text{H}_2\text{O})_4](\text{NO}_3)(\text{H}_2\text{O})_3$ (**1**): Yield: 73%. Anal. Calc. for $\text{C}_{18}\text{H}_{26}\text{Br}_2\text{N}_3\text{O}_{16}\text{Fe}_2$: C, 26.63; H, 3.23; N, 5.18; Fe, 13.76. Found: C, 25.81; H, 3.14; N, 5.31; Fe, 13.41%. Conductivity in DMF at 25 °C, $\Lambda = 64.5 \text{ S cm}^2 \text{ mol}^{-1} \text{ L}$.

$[\text{Fe}_2(\text{BrSA-Ile})_2(\text{H}_2\text{O})_4](\text{NO}_3)(\text{H}_2\text{O})_3$ (**2**): Yield: 76%. Anal. Calc. for $\text{C}_{26}\text{H}_{42}\text{Br}_2\text{N}_3\text{O}_{16}\text{Fe}_2$: C, 33.79; H, 4.58; N, 4.55; Fe, 12.08. Found: C, 34.71; H, 4.41; N, 4.67; Fe, 12.44%. Conductivity in DMF at 25 °C, $\Lambda = 64.0 \text{ S cm}^2 \text{ mol}^{-1} \text{ L}$.

Microanalyses were performed with a Fisons elemental analyzer, model EA1108, and with a Shimadzu atomic absorption spectrophotometer, model AA-6200. The infrared spectra (KBr pellets) were recorded using a Bruker spectrophotometer, model AMX300. The Mössbauer spectra of these complexes, as fine powder samples, were obtained with a conventional spectrometer with constant acceleration. The source was 10 mCi ^{57}Co in a Pd matrix. The gamma ray detection was carried out with a Reuter–Stokes detector connected to an Ortec amplifying and selecting system. A 1024 channel Canberra multichannel analyser was used for the data acquisition. The Mössbauer spectra were recorded at 298 K in the absence of an external magnetic field. The reported isomer shift values are relative to sodium nitroprusside. Electrochemical studies were done with a PAR 173 potentiostat and PAR 175 programmer, equipped with a digital coulometer model 179. Polarographic measurements were done with a BAS CV27 cyclic voltammetry setup. Molar conductance was measured at 25 °C on a Radiometer conductimeter, model CDM-83 with a CDC-304 electrode. Cyclic voltammograms of the complexes were recorded in DMF with $[\text{TBA}][\text{PF}_6]$ as supporting electrolyte in the potential range +1.3 to –1.8 V versus SCE. Ferrocenium was used as an internal reference. Electronic spectra were recorded on a Unicam II UV–Vis spectrophotometer. Variable temperature magnetic susceptibility data (5–300 K) were obtained with a CRYOGENICS Model S600 SQUID susceptometer–magnetometer, calibrated with $\text{Hg}[\text{Co}(\text{SCN})_4]$. The diamagnetic corrections were calculated from Pascal’s constants [18].

3. Results and discussion

The complexes can be considered as species with two six-coordinated iron centres, with the metal ions surrounded by water molecules, and the salicylideneimine ligand coordinated through the imine nitrogen and the phenolic oxygen, constituting a NO_5 donor set. Both metal ions are bridged by the carboxylate groups of the amino acids residues, Fig. 2.

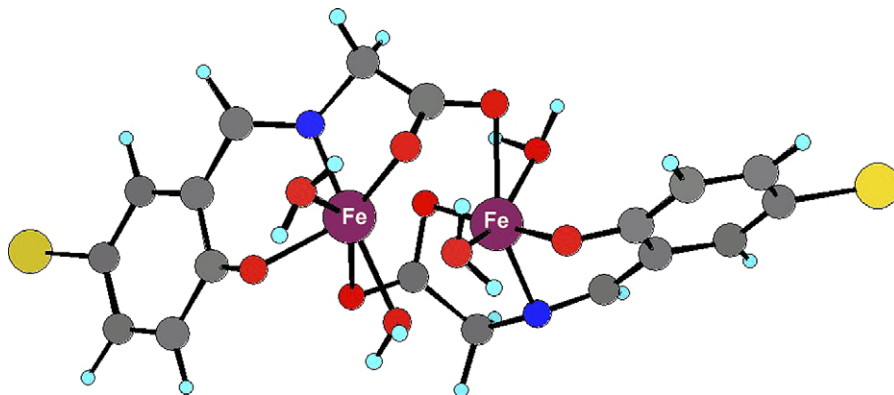


Fig. 2. Structures of dinuclear iron(II,III) complexes with Schiff bases derived from 5-bromosalicylaldehyde and α -amino acids ($R = \text{H}$, Sec-Bu).

3.1. Infrared and UV-Vis spectra

The mixed valence complexes show the same pattern for analogous vibrations. The vibration of the $-\text{C}=\text{N}$ bond in the complexes is displaced towards lower energies, in comparison with the free ligand (15 cm^{-1} for (1) and 21 cm^{-1} for (2)). The $-\text{C}-\text{O}_{\text{phenolic}}$ group band is displaced to higher energies ($\sim 30\text{ cm}^{-1}$ in both complexes). Two strong bands at $1362\text{--}1372$ and $1527\text{--}1529\text{ cm}^{-1}$, associated with symmetric and asymmetric stretching absorptions of the carboxylate group, also show a decrease in energy in respect to the free ligand. The difference between these bands is correlated with the coordination mode of the carboxylate ligands. For the free ligands the differences between ν_a and ν_s ($\Delta\nu$) of the carboxylate groups are 224 and 230 cm^{-1} for the glycine and isoleucine Schiff base ligands, respectively. In the complexes, $\Delta\nu$ has a value of about 170 cm^{-1} , indicative of a bridging carboxylate group between the two metal atoms [19–21]. The spectra of the two complexes show a broad band at 3400 cm^{-1} due to coordinated water molecules. The single absorption at 1383 cm^{-1} is indicative of an ionic nitrate group [21].

In agreement with the infrared data and reported assignments for analogous diiron(III) complexes [16], it is possible to infer that each iron ion in these mixed valence complexes has a hexa-coordinated environment, in which the metal ion is coordinated to two water oxygens, a phenol oxygen, an imine nitrogen and two carboxylate oxygen atoms; the latter groups bridging both iron atoms (Fig. 2).

The electronic spectra of the complexes are strongly dominated by the electronic transitions due to the iron-salicylaldiminate chromophores. The charge transfer bands, from phenolate to the metal, are of intermediate intensity, appear near 450 nm , and are responsible for the red-purple colour of the complexes. These transitions can be assigned to a charge transfer from the $p\pi$ orbital of the phenolic oxygen to the $d\pi$ orbital of the iron centre [22,23].

3.2. Mössbauer spectroscopy

To assign the oxidation states of the iron centres in these dinuclear complexes, Mössbauer spectroscopy was

used, since the isomer shift and the quadrupolar splitting can be related directly to populations of valence shell orbitals. Fig. 3 shows a representative spectrum and the fit of the data using least squares. The Mössbauer parameters obtained for the iron complexes are summarised in Table 1.

The Mössbauer spectra of both complexes exhibit two highly asymmetric quadrupole doublets. The integrated absorption intensities of the two spectral subcomponents show a 1:1 ratio, and therefore the relative amount of iron in both sites is the same.

For the first site of complex (1) the isomer shift (δ_1) is 0.51 mm s^{-1} and for complex (2) it is 0.56 mm s^{-1} . The quadrupolar splitting values (ΔE_{Q1}) are 0.91 mm s^{-1} for (1) and 0.96 mm s^{-1} for (2). These data correspond to high spin iron(III) ions ($S = 5/2$, ${}^6\text{A}_1$) [16,24–27]. For the second site, the chemical shifts (δ_2) are 1.40 mm s^{-1} for (1) and 1.41 mm s^{-1} for (2). The quadrupolar splitting (ΔE_{Q2}) is 2.68 mm s^{-1} for (1) and 2.65 mm s^{-1} for (2); these values correspond to high spin iron(II) ($S = 2$, ${}^5\text{T}_2$) [25–27].

On the other hand, complexes (1) and (2) have similar hyperfine parameters for site one. This allows us to assume that the coordination sphere and distortion of the octahedral geometry are the same for both complexes. The previous analysis can also be applied to the second site, since the hyperfine values for the two complexes are comparable. Furthermore, in these Fe(II,III) complexes, the iron(III) ion has a lower electronic density and a greater distortion of the octahedral geometry than in the analogous

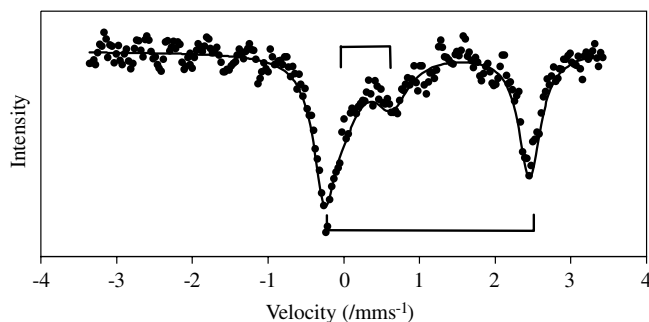


Fig. 3. Mössbauer spectrum for (1) at 300 K.

Table 1
Mössbauer parameters for dinuclear mixed valence complexes at 298 K

Complexes	I.S. ^a (mm s ⁻¹)		ΔE_Q^b (mm s ⁻¹)		A_1/A_2^c
	Site 1	Site 2	Site 1	Site 2	
(1)	0.51	1.39	0.91	2.67	1.05
(2)	0.56	1.41	0.96	2.65	1.32

The values of the chemical shifts are referred to sodium nitroprusside.

^a Isomer shift.

^b Quadrupolar splitting.

^c Area ratio.

Fe(III,III) complexes ($\delta = 0.61$ – 0.66 mm s⁻¹, $\Delta E_Q = 0.70$ – 0.76 mm s⁻¹).

Lippard et al. have shown that high spin iron(II) dinuclear complexes with carboxylate bridges have a smaller isomer shift when the coordination number is lower [28]. For example, iron (II) sites with coordination number four tend to have a smaller isomer shift (1.0–1.1 mm s⁻¹) compared with those with coordination number six (1.3 mm s⁻¹ approximately). The same authors also found that the carboxylate bridged diiron(II) species with a single N and variable number of O donor atoms present different isomer shifts. Iron(II) centres with a tetrahedral environment have an isomer shift of 1.04 mm s⁻¹. However diiron(II) complexes with an NO₄ environment in a square pyramidal geometry have an isomer shift of 1.12 mm s⁻¹, while in pentacoordinated complexes with a trigonal bipyramidal geometry the isomer shift is 1.19 mm s⁻¹. Finally, octahedral complexes with an NO₅ coordination sphere have an isomer shift of 1.35 mm s⁻¹. In our case, the Mössbauer data obtained for the two complexes show that the isomer shift for the iron(II) site is 1.40 mm s⁻¹, corroborating an octahedral arrangement for this type of iron centres. Consequently, it is correct to propose for complexes (1) and (2) a mixed valence (II,III) species with a pseudo-octahedral arrangement for each iron atom.

3.3. Cyclic voltammetry

The electrochemical behaviour of the dinuclear complexes was studied by cyclic voltammetry. The redox

Table 2
Electrochemical data for dinuclear mixed valence complexes^a

Complexes	Redox wave	E_{pa}	E_{pc}	ΔE	$E_{1/2}$	i_{pa}/i_{pc}
(1)	I	-0.18	-0.24	0.04	-0.21	0.45
	II	-0.43	-0.53	0.10	-0.48	1.07
	III	-0.90	-1.00	0.10	-0.95	1.17
(2)	I	-0.20	-0.24	0.04	-0.22	0.63
	II	-0.44	-0.56	-0.12	-0.50	0.76
	III	-0.92	-1.24	0.32	-1.13	0.76

^a Potential values are in volts and referred to SCE. E_{pa} and E_{pc} are the anodic and cathodic peak potentials respectively. $\Delta E = E_{pa} - E_{pc}$; $E_{1/2} = (E_{pa} + E_{pc})/2$.

parameters are summarised in Table 2. The redox processes were observed at essentially identical potentials for complex (1) and complex (2). This result is indicative of a similar electronic environment for the metal ions in both complexes. Fig. 4 shows the voltammogram of mixed valence complex (1). In the first cycle (reduction sweep), only two redox processes are seen; the first peak at -0.51 V can be attributed to the Fe(II,III)/Fe(II,II) redox process and the second peak at -0.90 V, that involves more than one electron, may be assigned to the reduction of the Fe(II,II) species. In the oxidation sweep, it is possible to observe three processes: the first one at -1.00 V, can be assigned to the regeneration of the Fe(II,II) species; the second process at -0.53 V involves the formation of the Fe(II,III) species, and the third process at -0.18 V can be assigned to the formation of the Fe(III,III) species. In the second cycle a new reduction process at -0.18 V corresponding to the Fe(III,III)/Fe(II,III) reduction process is observed. In summary, in the first cycle it is possible to find only two reduction processes and three oxidation processes, while after this cycle, three reduction and three oxidation processes are detected, with half wave potentials at $E_{1/2}^1 = -0.21$ V, $E_{1/2}^2 = -0.48$ V and $E_{1/2}^3 = -0.95$ V. Complex (2) shows a similar behaviour as complex (1), with half wave potentials at $E_{1/2}^1 = -0.22$ V, $E_{1/2}^2 = -0.50$ V and $E_{1/2}^3 = -1.13$ V.

The redox processes are quasireversible and correspond to a diffusion-controlled process. It is important to remark that under the same experimental conditions, the cyclic voltammograms for the free ligands do not present any redox process, and therefore all the redox process observed can be attributed to the metal centres.

Previous work on the substituent effect on the electrochemical potentials was done for a series of [FeIII-(X-SA)₂trien]⁺ complexes, (where SA = salicylaldehyde, trien = triethylamine, and X represents different substituents on the benzene ring, such as, H, NO₂, OCH₃, Br, Cl) [29,30]. The redox process in these complexes involves a one-electron transfer, which was assigned to the Fe(III)/Fe(II) reduction. The half wave potentials vary between -0.21 and -0.53 V versus SCE, depending on the substituent. For example, electron-donating groups such as OCH₃ make the metal centre more electron-rich thus hindering the reduction process. Electron-withdrawing groups, such as Cl, Br or NO₂, have an opposite effect on the reduction process [29–31].

A similar result is obtained for complexes (1) and (2) as seen in the second cycle; the bromine-substituted complexes have their redox processes at lower potentials than the analogous unsubstituted diiron(III) complexes. This difference may be attributed to the inductive effect of the bromine atom on the benzene ring. From the difference of the redox potentials, $E_2 - E_1 = (RT/F)\ln K$, the conproportionation constant K at 293 K of the following reaction can be calculated.



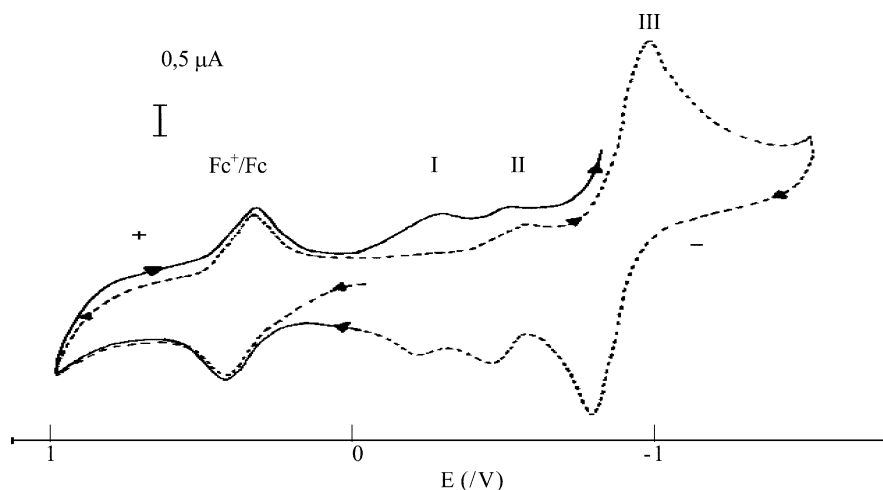


Fig. 4. Cyclic voltammogram of (1).

The K values obtained for the complexes were 3.7×10^4 and 5.4×10^4 for (1) and (2), respectively. These values are consistent with moderate electron coupling and charge delocalisation between the metal centres.

The degree of interaction between the two centres depends on the bridging ligand and on the nature of the metal. For example, a molybdenum complex with perfluorophthalate as bridging ligand presents a K value of 13. However, when the ligand is oxalate the K value is 5.4×10^4 ; the greater delocalisation is attributed to the shorter bridging group. On the other hand, when molybdenum is substituted by tungsten, in the oxalate complex, the K value is 1.3×10^{12} , that is, the extent of delocalisation is increased [32].

3.4. Magnetic susceptibilities

The magnetic susceptibilities of $[\text{Fe}_2(\text{L}_2(\text{H}_2\text{O})_4)(\text{NO}_3)(\text{H}_2\text{O})_3]$ were recorded over the temperature range 5–300 K. The plot of the reciprocal molar susceptibility versus temperature for complex (1) is shown in Fig. 5, and corresponds to a Curie–Weiss behaviour. The glycine-derived

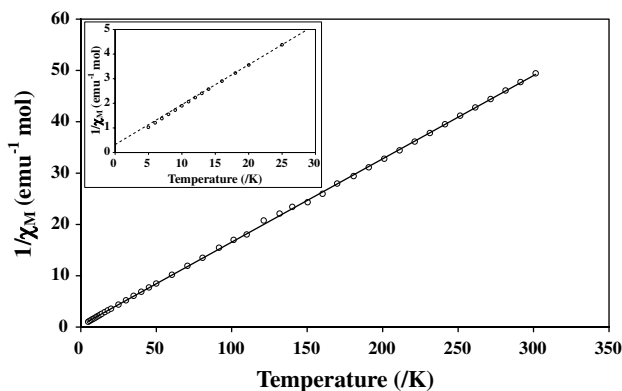


Fig. 5. Temperature dependence of the reciprocal molar susceptibility for (1).

Schiff base complex has an effective magnetic moment per molecule (μ_{eff}), which decreases from $6.82 \mu_{\text{B}}$ at 300 K to $5.96 \mu_{\text{B}}$ at 5 K. The trend is similar for (2), that is, μ_{eff} is $6.65 \mu_{\text{B}}$ per molecule at 300 K and decreases to $5.96 \mu_{\text{B}}$ at 5 K. For these complexes the μ_{eff} values at 300 K are lower than the expected spin-only value of $7.68 \mu_{\text{B}}$ for the moment of two independent high spin iron(III) and iron(II) ions ($S = 5/2$, $S = 2$). The decrease of μ_{eff} at lower temperature indicates that the two iron centres are weakly antiferromagnetically coupled.

The magnetic susceptibility of the mixed valence binuclear iron(II,III) complexes was analysed using the van Vleck equation, with a spin exchange Hamiltonian $\mathbf{H} = -2JS_1 \times S_2$, where $S_1 = 5/2$ and $S_2 = 2$. All the calculations were performed using a least-squares minimisation routine, where $\text{SSQ} = \sum_i [(\chi_i^{\text{obs}} - \chi_i^{\text{calc}})/\chi_i^{\text{obs}}]^2$. The parameter $R = \text{SSQ}/(n - p)$, where n is the number of experimental points and p is the number of parameters allowed to vary in the minimisation routine, is reported. The final magnetic parameters obtained for complexes (1) and (2) are $J = -0.17 \text{ cm}^{-1}$, $g = 2.62$, $\theta = -2.50$ and $J = -0.14 \text{ cm}^{-1}$, $g = 2.53$, $\theta = -2.23 \text{ K}$, respectively, indicating that the two iron ions are weakly antiferromagnetically coupled.

The results obtained for complexes (1) and (2), are comparable to those obtained for dinuclear iron(III) complexes with analogous ligands, in which the J values vary between -0.09 and -0.21 cm^{-1} as reported in previous work, and as shown in Table 3 [16].

On the other hand, these values can be also compared with those reported for other carboxylate-bridged complexes, in which the magnetic properties of the diiron complexes depend significantly on metal–metal distances, as well as on the nature of the other bridging ligands [30]. Table 3 presents the J values for a series of different dinuclear iron complexes with carboxylates bridged. Nevertheless, according to these data, it is possible to infer that the weak antiferromagnetic coupling interaction exhibited by complexes (1) and (2) can be explained by a large distance

Table 3
Magnetic parameters for carboxylate-bridged iron complexes

Complexes	Distance Fe...Fe (Å)	J (cm ⁻¹)	Ref.
<i>Fe^{II}-Fe^{III}</i>			
(1)		-0.17	this work
(2)		-0.14	this work
[Fe ₂ (salmp) ₂] ^{-a}	3.080	+8.6	[33]
[Fe ₂ (O ₂ CCH ₃) ₂ (TPA) ₂](BPh ₄) ₂ ^b	4.288	-1.0	[34]
[Fe ₂ (bpmp)(μ-O ₂ CC ₂ H ₅) ₂] ^{+c}	3.365	-2.5	[33]
[Fe ₂ (μ-OH)(μ-piv) ₂](ClO ₄) ₂ ^d	3.400	-12.9	[35]
<i>Fe^{II}-Fe^{II}</i>			
[Fe ₂ (μ-XDK)(μ-O ₂ CPh)- (ImH) ₂ (O ₂ CPh)(MeOH)] ^e	3.609	-0.51	[36]
[Fe ₂ (μ-O ₂ CAR) ₂ (O ₂ CAR) ₂ L ₂] ^f	4.218	-0.90	[19]
[Fe ₂ (O ₂ CH) ₄ (BIPhMe) ₂] ^g	3.575	-0.16	[37]
[Fe ₂ O(O ₂ CH) ₄ (BIPhMe) ₂] ^g	3.211	-31.0	[37]
<i>Fe^{III}-Fe^{III}</i>			
[Fe ₂ L ₂ (H ₂ O) ₄](NO ₃)(H ₂ O) ₃ ^h		-0.12	[16]
[Fe ₂ L ₂ (H ₂ O) ₄](NO ₃)(H ₂ O) ₃ ^h		-0.12	[16]
[Fe ₂ (O ₂ CCH ₃) ₂ L ₂](ClO ₄) ⁱ	4.482	-1.5	[38]
[Fe ₂ (OH)(OAc) ₂ (HBpz ₃) ₂] ^j	3.439	-17.0	[39]
[Fe ₂ (μ-O)(μ-pivalate) ₂](ClO ₄) ₂ ^d	3.123	-111.0	[35]
[Fe ₂ O(OAc) ₂ (HBpz ₃) ₂] ^j	3.145	-121.0	[39]

^a salmp = bis(salicylidenamino)-2-methylphenolate.

^b TPA = tris(2-pyridylmethyl)amine.

^c bpmp = 2,6-bis[bis(pyridylmethyl)aminomethyl]-4-methylphenolate.

^d piv = pivalic acid.

^e KDX = Kemp's derived triacid.

^f L = C₅H₅N.

^g BIPhMe = 2,2'-bis-(1-methylimidazolyl)phenyl methoxymethane.

^h L = salicylideneamino acids.

ⁱ L = *N,N'*-dimethyl-*N,N'*-bis(2-pyridylmethyl ethane)-1,2-diamine.

^j HBpz₃ = hydrotris(1-pyrazolyl)borato.

between both metal centres, and by the absence of a more efficient exchange pathway such as oxo, hydroxo or alkoxo bridges [16,19,33–39].

4. Conclusions

Two hexacoordinated mixed valence complexes, with an NO₅ coordination sphere, were obtained with Schiff base ligands derived from 5-bromosalicylaldehyde and glycine (1) or isoleucine (2). The FTIR data show that each ligand is coordinated to the metal centres through the imine nitrogen, phenolic oxygen and carboxylate groups, which also act as bridging ligands between both iron atoms. The remaining coordination positions are occupied by water molecules.

With Mössbauer spectroscopy it was possible to find two sites for the iron atoms. The isomer shifts and quadrupolar splittings for both sites correspond to high spin Fe(II) and Fe(III). The hyperfine values obtained for both complexes are comparable, and indicate that these complexes have a greater distortion than analogous Fe(III,III) complexes.

From cyclic voltammetry the presence of a mixed valence Fe(II,III) complex was confirmed. In the case of the studied bromine-substituted ligands, the complexes

show lower values for all the redox potentials as compared to the complexes with unsubstituted ligands. This difference is attributed to the presence of the electron-withdrawing groups on the aromatic ring.

Magnetic susceptibility data for complexes (1) and (2) show that the two iron centres have a weak antiferromagnetic exchange coupling, which is principally attributed to three factors: (i) the strong distortion of the octahedral geometry, (ii) relatively large Fe-Fe distance and (iii) the absence of a more efficient exchange pathway. The J values obtained for both complexes are comparable to other dinuclear iron complexes with carboxylate bridges.

From the complete analyses done in this work, it is important to remark that when 5-bromosalicylaldehyde is used to form the Schiff base, a mixed valence species is obtained. Apparently the electronic effect of the bromine atom in the aromatic ring stabilises a mixed valence species.

Acknowledgement

Financial support for this work provided by FONDECYT 2960043, FONDAP 11980002 and PICS 922 Grants is gratefully acknowledged.

References

- [1] A.L. Feig, S.J. Lippard, Chem. Rev. 94 (1994) 759.
- [2] E.I. Solomon, T.C. Brunold, M.I. Davis, J.N. Kemsley, S.K. Lee, N. Lehnert, F. Neese, A.J. Skulan, Y.S. Yang, J. Zhou, Chem. Rev. 100 (2000) 235.
- [3] B.J. Wallar, J.D. Lipscomb, Chem. Rev. 96 (1996) 2625.
- [4] M. Merx, D.A. Kopp, M.H. Szazinsky, J.L. Blazyk, J. Müller, S.J. Lippard, Angew. Chem., Int. Ed. Engl. 40 (2001) 2782.
- [5] E.Y. Tshuva, S.J. Lippard, Chem. Rev. 104 (2004) 987.
- [6] R.H. Holm, P. Kennepohl, E.I. Solomon, Chem. Rev. 96 (1996) 2239.
- [7] E.I. Solomon, D.W. Randall, T. Glaser, Coord. Chem. Rev. 200–202 (2000) 595.
- [8] S.J. Lippard, Angew. Chem., Int. Ed. Engl. 27 (1988) 344.
- [9] F. Dianzhong, W. Bo, Trans. Met. Chem. 18 (1993) 101.
- [10] R.E. Norman, S. Yan, G. Backes, J. Ling, S. O'Connor, J.H. Zhang, L. Que, J. Am. Chem. Soc. 112 (1990) 1554.
- [11] W. Kwik, A.W.N. Tay, Tetrahedron 9 (1990) 1293.
- [12] L. Canali, D.C. Sherrington, Chem. Soc. Rev. 28 (1999) 85.
- [13] Y.Z. Voloshin, O.A. Varzatskii, E. Tkachenko, Y.A. Maletin, S.P. Degtyarov, D.I. Kochubey, Inorg. Chim. Acta 255 (1997) 255.
- [14] (a) G. Blondin, J. Girerd, Chem. Rev. 90 (1990) 1359;
(b) D.M. Kurtz, Chem. Rev. 90 (1990) 585;
(c) J. Vincent, G. Olivier, B. Averill, Chem. Rev. 90 (1990) 1447;
(d) S. Lippard, Angew. Chem., Int. Ed. Engl. 27 (1988) 344.
- [15] A. Nivorozhkin, P. Mialane, R. Davydov, J. Guilhem, J.J. Girerd, S. Styring, Inorg. Chem. 36 (1997) 846.
- [16] V. Paredes-García, R.O. Latorre, E. Spodine, Polyhedron 23 (2004) 1869.
- [17] L. Casella, M. Gullotti, A. Pintar, L. Messori, M. Györ, Inorg. Chem. 26 (1987) 1031.
- [18] A. Earnshaw, Introduction to Magnetochemistry, Academic Press, London, 1968.
- [19] D. Lee, S.J. Lippard, Inorg. Chem. 41 (2002) 2704.
- [20] D. Sattari, E. Alipour, S.J. Shirani, Inorg. Biochem. 45 (1992) 115.
- [21] K. Nakamoto, Infrared and Raman Spectra of Inorganic Coordination Compounds, Wiley, New York, 1986, pp. 232.

- [22] K. Ramesh, R. Mukherjee, *J. Chem. Soc., Dalton Trans.* (1992) 83.
- [23] D. Cook, D. Cummins, E.D. McKenzie, *J. Chem. Soc., Dalton Trans.* (1976) 1369.
- [24] S. Herold, S.J. Lippard, *Inorg. Chem.* 36 (1997) 50.
- [25] G. Long, *Mössbauer Spectroscopy Applied to Inorganic Chemistry*, Plenum Press, New York, 1984, p. 43.
- [26] L. May, *An Introduction to Mössbauer Spectroscopy*, Plenum Press, New York, 1971.
- [27] V.I. Gol'danskii, R.H. Herber, *Chemical Applications of Mössbauer Spectroscopy*, Academic Press, New York, 1968.
- [28] S. Yoon, S.J. Lippard, *J. Am. Chem. Soc.* 127 (2005) 8386.
- [29] A. Bettelheim, R. Paresh, O. Dozen, *J. Electrochem. Soc.* 129 (1982) 2247.
- [30] K. Kadish, C.H. Su, J. Wilson, *Inorg. Chem.* 21 (1982) 2312.
- [31] D. Lee, J.L. DuBois, B. Pierce, B. Hedman, K.O. Hodgson, M.P. Hendrich, S.J. Lippard, *Inorg. Chem.* 41 (2002) 3172.
- [32] A.W. Bott, *Curr. Separ.* 16 (1997) 61.
- [33] G. Peng, J. van Elp, H. Hang, L. Que Jr., W.H. Armstrong, S.P. Cramer, *J. Am. Chem. Soc.* 117 (1995) 2515.
- [34] S. Ménage, Y. Zang, P. Hendrich, L. Que Jr., *J. Am. Chem. Soc.* 114 (1992) 7786.
- [35] U. Bossek, H. Hummel, T. Weyhermüller, E. Bill, K. Wieghardt, *Angew. Chem., Int. Ed. Eng.* 34 (1995) 2642.
- [36] (a) S. Herold, S.J. Lippard, *J. Am. Chem. Soc.* 119 (1997) 145;
(b) V. Grillo, R. Hanson, W.H. Trevor, L. Gaham, K. Murray, B. Molubaraki, *J. Chem. Soc., Dalton Trans.* (1997) 305.
- [37] W.B. Tolman, S. Liu, J.G. Bensten, S.J. Lippard, *J. Am. Chem. Soc.* 113 (1991) 152.
- [38] R. Hazell, K.B. Jensen, J. McKenzie, H. Toftlund, *J. Chem. Soc., Dalton Trans.* (1995) 707.
- [39] W.H. Armstrong, A. Spool, G.C. Papaefthymiou, R.B. Frankel, S.J. Lippard, *J. Am. Chem. Soc.* 106 (1984) 3653.